Science of the Total Environment 755 (2021) 143562

Contents lists available at ScienceDirect

Science of the Total Environment

journal homepage: www.elsevier.com/locate/scitotenv

An approach for decomposing river water-quality trends into different flow classes

Qian Zhang [a,*], James S. Webber [b], Douglas L. Moyer [b], Jeffrey G. Chanat [b]

[a] University of Maryland Center for Environmental Science, Chesapeake Bay Program Office, Annapolis, MD, USA
[b] U.S. Geological Survey, Virginia and West Virginia Water Science Center, Richmond, VA, USA

HIGHLIGHTS

- The FN_{2Q} approach can decompose water-quality trends into different flow classes.
- The utility of FN_{2Q} is demonstrated with a case study on TN in a 4232 km^2 watershed.
- Wastewater reductions have likely led to the decline in TN flux under low flows.
- A high-flow increase in TN flux around 2007 was likely due to transport of particulate N.
- FN_{2Q} (and the published code) can easily be applied to monitoring records elsewhere.

GRAPHICAL ABSTRACT

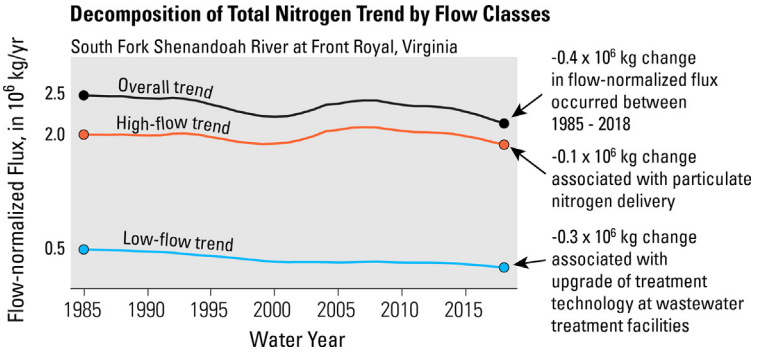

ARTICLE INFO

Article history:
Received 5 August 2020
Received in revised form 29 October 2020
Accepted 3 November 2020
Available online 7 November 2020

Editor: Ashantha Goonetilleke

Keywords:
Water quality
Trend analysis
Flow classes
WRTDS
Nitrogen
Wastewater

ABSTRACT

A number of statistical approaches have been developed to quantify the overall trend in river water quality, but most approaches are not intended for reporting separate trends for different flow conditions. We propose an approach called FN_{2Q}, which is an extension of the flow-normalization (FN) procedure of the well-established WRTDS ("Weighted Regressions on Time, Discharge, and Season") method. The FN_{2Q} approach provides a daily time series of low-flow and high-flow FN flux estimates that represent the lower and upper half of daily riverflow observations that occurred on each calendar day across the period of record. These daily estimates can be summarized into any time period of interest (e.g., monthly, seasonal, or annual) for quantifying trends. The proposed approach is illustrated with an application to a record of total nitrogen concentration (632 samples) collected between 1985 and 2018 from the South Fork Shenandoah River at Front Royal, Virginia (USA). Results show that the overall FN flux of total nitrogen has declined in the period of 1985–2018, which is mainly attributable to FN flux decline in the low-flow class. Furthermore, the decline in the low-flow class was highly correlated with wastewater effluent loads, indicating that the upgrades of treatment technology at wastewater treatment facilities have likely led to water-quality improvement under low-flow conditions. The high-flow FN flux showed a spike around 2007, which was likely caused by increased delivery of particulate nitrogen associated with sediment transport. The case study demonstrates the utility of the FN_{2Q} approach toward not only characterizing the changes in river water quality but also guiding the direction of additional analysis for capturing the underlying drivers. The FN_{2Q} approach (and the published code) can easily be applied to widely available river monitoring records to quantify water-quality trends under different flow conditions to enhance understanding of river water-quality dynamics.

* Corresponding author.
E-mail address: qzhang@chesapeakebay.net (Q. Zhang).

https://doi.org/10.1016/j.scitotenv.2020.143562

1. Introduction

Rivers are an important component of the Earth's ecosphere. Unfortunately, anthropogenic activities, particularly nutrient pollutions, have caused widespread water-quality degradation in rivers around the world, which in turn have negative impacts on the environmental status of receiving waterbodies such as lakes, estuaries, and oceans (Seitzinger et al., 2010; Boesch, 2019; Malone and Newton, 2020). To inform management efforts for protecting and restoring water quality, it is critical to understand changes that have taken place in rivers. This requires both monitoring of river water quality and development of analytical approaches for extracting information from the monitoring data.

At many river monitoring locations, flow discharges are recorded at 15-min intervals and can be aggregated to daily values. However, concentrations of water-quality constituents (e.g., nitrogen, phosphorus, and sediment) are sampled at much lower frequencies, which range between monthly and weekly (e.g., Chanat et al., 2016; Sprague et al., 2017). At some locations, routine water-quality samples are supplemented by additional, targeted samples during high-flow conditions, which are helpful for capturing water-quality signals across different hydrologic conditions. For example, in the Chesapeake Bay watershed (USA), monitoring stations have at least 20 water-quality samples per year, which include 12 regular monthly samples and eight targeted stormflow samples (Chanat et al., 2016). These monitoring data, as well as those collected at other locations in the United States, contain critical information regarding the conditions of the monitored rivers, which can be accessed through national databases such as the U.S. Geological Survey (USGS) National Water Information System (https://waterdata.usgs.gov/nwis). In general, water-quality data are intrinsically variable over years and seasons due to natural factors (e.g., hydro-climatic cycles, biogeochemical processes) and anthropogenic drivers (e.g., land-use changes, management actions) (Zhang et al., 2016a; Lintern et al., 2018; Guo et al., 2019; Manning et al., 2020; Stets et al., 2020). Consequently, it is usually a challenge to effectively filter out the underlying trend signal in the observed time series from the variability related to time, season, and discharge.

Several analytical approaches have been developed to quantify trends in hydrologic time series. One traditional approach is the nonparametric Mann-Kendall test, which is designed for detecting monotonic trends (Kendall, 1975). An important adaptation of this approach is the seasonal Kendall test, which is applicable to time series with seasonality, missing values, and/or below detection-limit values (Hirsch et al., 1982). Associated with these approaches are the Sen's slope (Sen, 1968) and the seasonal Sen's slope (Hirsch et al., 1982), respectively, which quantify the trend magnitude. For more complete surveys of trend approaches, readers are referred to Hirsch et al. (1991), Esterby (1996), and Lloyd et al. (2014). More recently, several approaches were developed to accommodate non-linear and/or non-monotonic trends. For example, the seasonal trend decomposition approach can decompose a time series to a seasonal component, a nonlinear trend component, and a residual component (Cleveland et al., 1990; Qian et al., 2000; Stow et al., 2015). The generalized additive model (GAM) can account for seasonality, nonlinearity, and interactions between covariates (Hastie and Tibshirani, 1990; Murphy et al., 2019; Yang and Moyer, 2020).

Another recent approach is the Weighted Regressions on Time, Discharge, and Season (WRTDS) (Hirsch et al., 2010), which is also the focus of this research. WRTDS not only provides estimates of concentration and flux for each day in the period of record, but also quantifies temporal trends of concentration and flux. The trends are estimated with a procedure called "flow-normalization (FN)," which integrates the full range of riverflow for each calendar date of the year, thereby largely removing the effects of inter-annual variability in riverflow. Since its publication, WRTDS FN has been used to quantify water-quality trends, including nitrogen, phosphorus, sediment, carbon, and chlorophyll-*a* (Moyer et al., 2012; Zhang et al., 2015; Stackpoole et al., 2017; Zhang and Blomquist, 2018; Oelsner and Stets, 2019).

While the above approaches are widely accepted as a means of estimating the overall trend in the observed water-quality data, systematic decomposition of such trends into compartments representing particular ranges of flow conditions is more problematic. Conceptually, river water-quality signals reflect the contribution of waters from different compartments of the watershed, namely, surface runoff, soil interflow, and groundwater flow (Burns et al., 2001; Chanat et al., 2002; Botter et al., 2020; Zhi and Li, 2020). The availability of a given constituent may differ among these compartments and vary over time in response to atmospheric and hydrologic conditions, biogeochemical cycling, and human disturbance. Many of these factors also influence the relative contribution by each compartment to the total riverflow over time. Therefore, trend signals under different flow conditions can reveal nuanced insights into overall water-quality dynamics. For example, the effect of a management intervention that reduces nutrients during baseflow may be challenging to detect without the ability to parse water-quality trends by riverflow. Toward that end, an intuitive solution is to repeatedly apply one of the established trend approaches to observations collected under different flow conditions. For example, the segmented regression analysis approach by Murdoch and Shanley (2006) applies the linear regression approach to segmented data to quantify trends at specific flow levels, including 5th (low-flow), 50th (median-flow) and 95th (high-flow) percentiles. Similarly, Fanelli et al. (2019) used the estimated concentration regression surface from WRTDS to quantify the period-of-record changes in concentration at the 5th and 95th percentile flows to represent low-flow and high-flow trends, respectively. While these approaches certainly provide useful information on water-quality dynamics, they are specific and sensitive to selected flow levels.

The main objective of this research is to develop an approach for quantifying river water-quality trends under different flow conditions. The proposed approach, named FN_{2Q}, is an extension of the standard flow-normalization approach in WRTDS (Hirsch et al., 2010). WRTDS was chosen for three reasons. First, WRTDS generally can offer improved estimates than prior regression-based approaches (e.g., Cohn et al., 1989), because it does not assume homoscedasticity of model errors, fixed seasonal variations in concentration, or fixed concentration-discharge relationship (Moyer et al., 2012; Hirsch, 2014; Chanat et al., 2016; Lee et al., 2016; Zhang et al., 2016b; Lee et al., 2019). An in-depth discussion on the accuracy of WRTDS is beyond the scope of this work; readers are referred to the references above. Second, WRTDS can simultaneously estimate, store, and visualize water-quality patterns for different times and discharges. This is best represented by a WRTDS product called "concentration regression surface", which shows estimated concentration as functions of time and discharge. (An example concentration regression surface will be provided in Section 3.1.) In comparison, other approaches (including those listed above) typically cannot produce such a comprehensive description of water-quality signals. Third, WRTDS has already been widely used in national and regional assessments of water-quality changes and trends (e.g., Chanat et al., 2016; Murphy and Sprague, 2019; Oelsner and Stets, 2019; Moyer and Langland, 2020; Stets et al., 2020). Thus, FN_{2Q} adds a natural extension to these studies toward understanding river water-quality dynamics.

The unique contribution of FN_{2Q} is to quantify separate high-flow and low-flow trends for a water-quality constituent at a given river monitoring location using the well-established WRTDS framework. While WRTDS FN estimates the overall trend in the water-quality time series, FN_{2Q} estimates two separate trends, one each for low-flow and high-flow conditions. Importantly, since these two trend estimates are derived from the same concentration regression surface, they sum together to return the original trend estimate from the standard FN approach. In fact, FN_{2Q} is implemented utilizing existing functions in the *EGRET* (Exploration and Graphics for RivEr Trends) package (Hirsch and De Cicco, 2015). The key difference between the two approaches is that FN considers the full set of discharges occurring on each calendar

date in the period of record, whereas FN_{2Q} considers the upper half and the lower half of those discharges to represent high-flow and low-flow conditions, respectively. Also, we note that FN_{2Q} can be modified to accommodate other user-specified flow classes.

As is the case with WRTDS, the FN_{2Q} extension can easily be applied to widely available river monitoring records to quantify water-quality trends under different flow conditions, thereby enhancing understanding of river water-quality dynamics. Thus, the R code for implementing FN_{2Q} is made available to readers through Webber and Zhang (2020), which also contains daily FN_{2Q} estimates for several water-quality constituents at the Chesapeake Bay nontidal monitoring network stations.

2. Methods and data

2.1. WRTDS FN

WRTDS and its standard FN procedure are fully described in Hirsch and De Cicco (2015). In brief, WRTDS is designed for estimating daily concentrations and fluxes based on sparse (e.g., monthly, weekly) water-quality concentration samples. It uses time, discharge, and season as explanatory variables:

$$ln(C_i) = \beta_{0,i} + \beta_{1,i} t_i + \beta_{2,i} ln(Q_i) + \beta_{3,i} sin(2\pi t_i) + \beta_{4,i} cos(2\pi t_i) + \varepsilon_i \quad (1)$$

where t_i is time in decimal years, C_i is daily concentration at time t_i, Q_i is daily discharge at time t_i, $\beta_{0,i} \sim \beta_{4,i}$ are fitted coefficients, and ε_i is the error term. Unlike other established approaches, WRTDS develops a unique model (Eq. (1)) for each day in the period of record, and hence it allows the concentration-discharge relations to change over time, discharge, and season.

Operationally, WRTDS establishes a set of evenly spaced grid points on a surface defined by t and ln(Q) (Hirsch and De Cicco, 2015). Fig. 1a provides an example for water years 1985 through 2018, which corresponds to the case study in Section 3. For the x-axis (i.e., t), grid values are spaced 1/16th of a year apart from the first year to the last year of the record. For the y-axis (i.e., ln(Q)), 14 grid values are spaced evenly in log space from 5% below the minimum daily Q to 5% above the maximum daily Q in the period of record. At each grid point, WRTDS evaluates all available concentration samples and selects at least 100 samples

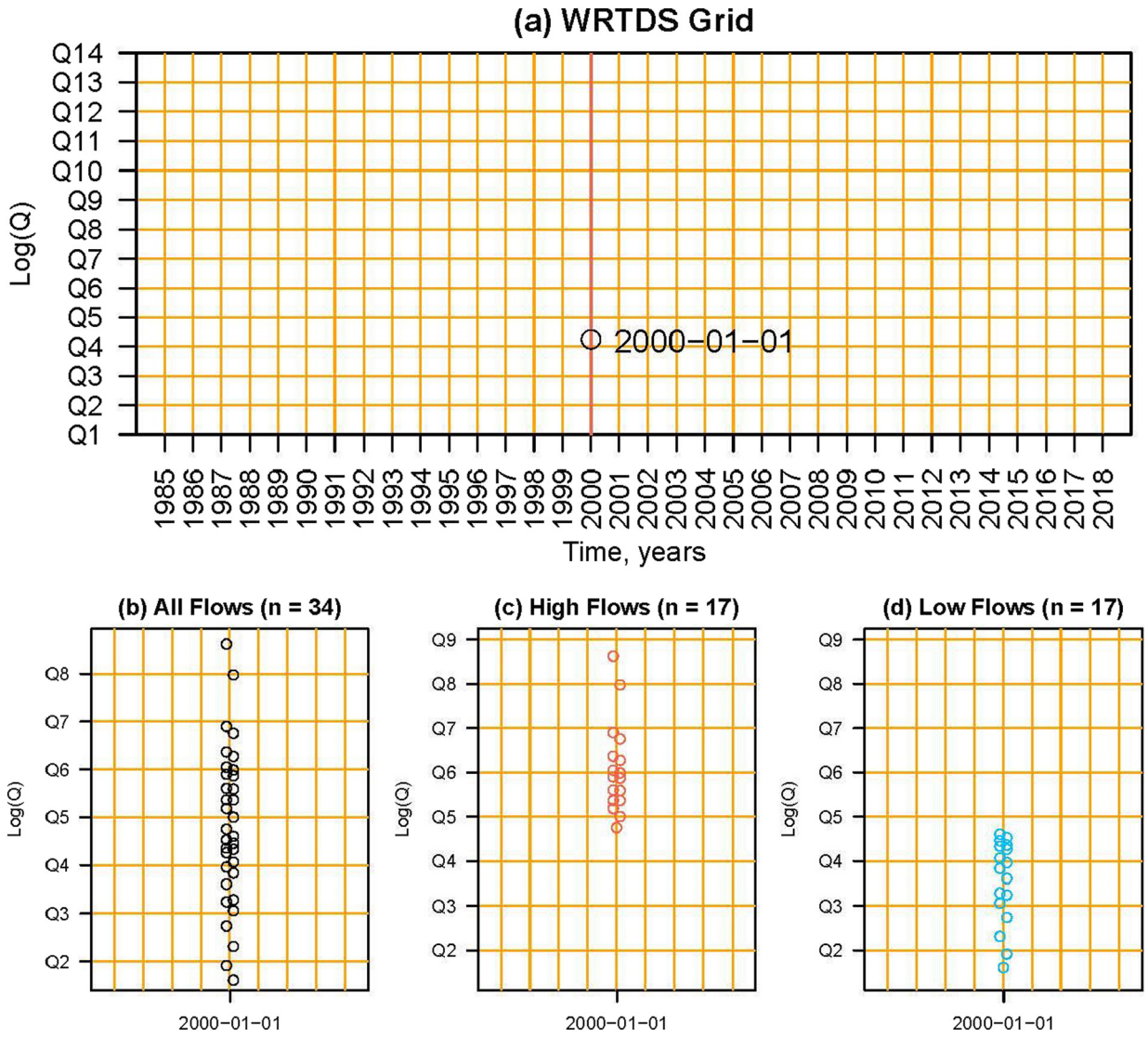

Fig. 1. The WRTDS concentration regression surface and FN estimation. (a) The grid formed by time (x-axis) and discharge (y-axis). On the x-axis (i.e., t), grid values are spaced 1/16th of a year apart in water years 1985 through 2018 (i.e., 1985-10-01 to 2018-09-30). For visual clarity, only the first vertical line of each year is shown. On the y-axis, 14 grid values are spaced evenly in log space from 5% below the minimum daily Q to 5% above the maximum daily Q in the period of record. For the estimation date of 2000-01-01, the standard FN considers all discharge values that occurred on January 1 in the period of record, whereas FN_{2Q} considers the top half (panel c) and bottom half (panel d) of these values to conduct the high-flow and low-flow estimation, respectively. Points in (b) - (d) are slightly adjusted along the x-axis to reduce overlap.

that are sufficiently close to that grid point in three dimensions, namely, time, discharge, and season. These selected samples are used to fit Eq. (1) and the fitted coefficients are used to estimate ln(C) for that grid point by substituting its values of t and $ln(Q)$. Then, a bilinear interpolation is implemented among all grid points, resulting in a concentration regression surface as functions of t and $ln(Q)$. (An example concentration regression surface is provided in Section 3.1.)

The concentration regression surface is the foundation for deriving two different versions of daily estimates by WRTDS, namely, true-condition (actual) estimates and FN estimates. Taking the date of 2000-01-01 as an example, its true-condition concentration estimate can be extracted from the concentration regression surface using $t =$ 2000-01-01 and $\ln(Q) = ln(Q_{2000\text{-}01\text{-}01})$ – see the black open circle in Fig. 1a. This concentration estimate can be multiplied by $Q_{2000\text{-}01\text{-}01}$ to calculate the true-condition flux estimate for that date.

By contrast, the FN estimate is obtained by using the full set of discharges occurring on the calendar date, thereby removing the effects of inter-annual variability in riverflow. Taking the date of 2000-01-01 as an example, the FN procedure first finds all discharges that have occurred on its calendar date (i.e., January 1st) in the period of record, as illustrated in Fig. 1b. For a period of record between 1985 and 2018, this results in a total of 34 discharge values that vary over the years, with each value considered one realization of discharge for January 1. Let j be the index of a certain year in the period of record, i.e., $j = 1$ for 1985-01-01, $j = 2$ for 1986-01-01, …, $j = 34$ for 2018-01-01. For each Q_j, we assign $t =$ 2000-01-01 (fixed) and $\ln(Q) = ln(Q_j)$ to the concentration regression surface to extract the concentration estimate C_j. Then, the FN estimate of concentration (C_{FN}) is calculated as the average of all 34 C_j estimates:

$$C_{FN} = \frac{1}{34}\sum_{j=1}^{34} C_j \tag{2}$$

Similarly, the FN estimate of flux (F_{FN}) is calculated as the average of all 34 flux estimates:

$$F_{FN} = \frac{1}{34}\sum_{j=1}^{34} C_j Q_j \tag{3}$$

For each day in the period of record, the above procedure is repeated to obtain complete daily records of true-condition and FN estimates for both concentration and flux, which can be aggregated to obtain monthly, seasonal, and annual estimates.

2.2. WRTDS FN_{2Q}

The concentration regression surface is also the foundation of the proposed FN_{2Q} approach. While FN considers the full set of discharges occurring on the calendar date to obtain the overall FN estimate, FN_{2Q} considers the upper half and the lower half of those discharges to obtain the FN estimates for high and low flows, respectively (Fig. 1b–d). For the example above, FN_{2Q} also starts by pooling all discharges that have occurred on January 1st between 1985 and 2018, resulting in the same set of 34 discharge values used to generate FN estimates. Then, FN_{2Q} ranks these values from the largest to the smallest. Let k be the index of these ranked values, with $Q_{k=1}$ as the maximum value and $Q_{k=34}$ as the minimum value. For each Q_k, we assign $t =$ 2000-01-01 (fixed) and $\ln(Q) = ln(Q_k)$ to the concentration regression surface to obtain its concentration estimate C_k.

In FN_{2Q}, the overall FN estimate of concentration and the overall FN estimate of flux (F_{FN_TOTAL}) can be calculated in the same manner as in the standard FN approach, and they are exactly the same as those obtained from the standard FN approach (Eqs. (2)–(3)):

$$C_{FN\_TOTAL} = \frac{1}{34}\sum_{k=1}^{34} C_k \tag{4}$$

$$F_{FN\_TOTAL} = \frac{1}{34}\sum_{k=1}^{34} C_k Q_k \tag{5}$$

In addition, FN_{2Q} calculates the high-flow FN estimate of concentration (C_{FN_HIGH}) using C_k estimates corresponding to the top half of the 34 discharges (i.e., $Q_{k=1}$–$Q_{k=17}$; see Fig. 1c).

$$C_{FN\_HIGH} = \frac{1}{17}\sum_{k=1}^{17} C_k \tag{6}$$

Also, FN_{2Q} calculates the low-flow FN estimate of concentration (C_{FN_LOW}) using C_k estimates corresponding to the bottom half of the 34 discharges (i.e., $Q_{k=18}$–$Q_{k=34}$; see Fig. 1d).

$$C_{FN\_LOW} = \frac{1}{17}\sum_{k=18}^{34} C_k \tag{7}$$

Then, the high-flow and low-flow FN estimates of flux are calculated as follows:

$$F_{FN\_HIGH} = \left(\frac{1}{17}\sum_{k=1}^{17} C_k Q_k\right) * \left(\frac{17}{34}\right) \tag{8}$$

$$F_{FN\_LOW} = \left(\frac{1}{17}\sum_{k=18}^{34} C_k Q_k\right) * \left(\frac{17}{34}\right) \tag{9}$$

Note that the averages in Eqs. (8) and (9) are multiplied by the proportion of allocated discharge values (i.e., 17 for the top and bottom halves of the total 34 values), such that the following relation holds true, which connects the FN_{2Q} and FN approaches:

$$F_{FN} = F_{FN\_TOTAL} = F_{FN\_HIGH} + F_{FN\_LOW} \tag{10}$$

Note that a similar relation does not hold true for FN concentrations.

Among all calendar dates, two special ones are February 28th and 29th, which have 34 and 8 discharge values in the period of 1985–2018. For these two dates, FN_{2Q} uses the combination of the 42 values to represent the flow distributions and allocates 21 values to each flow class. This handling of leap years is consistent with that currently implemented in WRTDS.

For records spanning an odd number of years (say, 35), FN_{2Q} allocates one more value to the high-flow class than to the low-flow class – i.e., $Q_{k=1}$–$Q_{k=18}$ for the high-flow class and $Q_{k=19}$–$Q_{k=35}$ for the low-flow class. For flux decomposition, Eq. (10) becomes:

$$F_{FN\_TOTAL} = F_{FN\_HIGH} + F_{FN\_LOW} = \left(\frac{1}{18}\sum_{k=1}^{18} C_k Q_k\right) * \left(\frac{18}{35}\right) + \left(\frac{1}{17}\sum_{k=19}^{35} C_k Q_k\right) * \left(\frac{17}{35}\right) \tag{11}$$

Like FN, FN_{2Q} is run to obtain FN estimates of concentration and flux for each day in the period of record. These daily estimates can be summed to obtain monthly, seasonal, and annual estimates and associated trends can be calculated. For our case study, we chose to present the seasonal fluxes by growing and non-growing seasons (Section 3). In this regard, we note that the daily estimates from FN and FN_{2Q} can be summed to obtain aggregated fluxes for other user-specified seasons.

By default, the proposed FN_{2Q} approach uses the median flow of each calendar date to define the low-flow and high-flow classes. This choice serves two purposes. First, the two flow classes cover the entire range of the flow distribution, such that their corresponding FN estimates sum exactly to the FN estimates from the standard FN approach (Eq. (10)). Second, the two flow classes each contain ~50% of discharge values for each calendar date. We note that the FN_{2Q} approach can be modified to accommodate other user-specified flow classes. However, we recommend at least several discharge values in each flow class for appropriately implementing the FN computation. For example, if the high-flow class is defined as the 95th percentile or above, a 20-year

record would result in only one value for that flow class for each calendar date, which is not appropriate for running FN.

The WRTDS Bootstrap Test (wBT) (Hirsch et al., 2015) can be adapted to quantify the uncertainties of the flux estimates from the FN_{2Q} approach. In brief, the original water-quality concentration samples are resampled 100 times using a "block bootstrap" method. Each of the 100 replicates is analyzed using the FN_{2Q} approach to obtain daily flux estimates for all flows, low flows, and high flows, respectively. For each realization, the daily estimates are aggregated to annual estimates and the period-of-record change is computed. From the 100 realizations, the likelihood of a downward trend (i.e., an improving condition) can be calculated (Hirsch et al., 2015). For example, the likelihood of a downward trend is 100% if the period-of-record change in annual flux is negative in all 100 realizations. The above steps are included in our R code (Webber and Zhang, 2020), which utilizes existing functions in the *EGRETci* (Exploration and Graphics for RivEr Trends Confidence Intervals) package (Hirsch et al., 2015).

2.3. Case study

Here we demonstrate the utility of the FN_{2Q} approach toward providing new insights into changes in river water quality. We use a case study on total nitrogen (TN) collected from the South Fork Shenandoah River at Front Royal, Virginia (USGS ID 01631000) (Fig. 2). This site drains 4232 km^2 of mostly forested and agricultural land from four Virginia counties. Between 1985 and 2018, natural land has remained stable, representing 60% of the watershed. Agricultural land has reduced from 32% to 28%, whereas developed land has expanded from 8% to 12% in the same period. Cattle and poultry production are the dominant agricultural activities in the watershed (Keisman et al., 2018). Most urban land surrounds the cities of Harrisonburg, Waynesboro, and Staunton. The North, Middle, and South Rivers come together about halfway up the watershed to form the South Fork of the Shenandoah River. The South Fork flows north for approximately 160 km, confined by the Blue Ridge Mountains to the east and Massanutten Mountain to

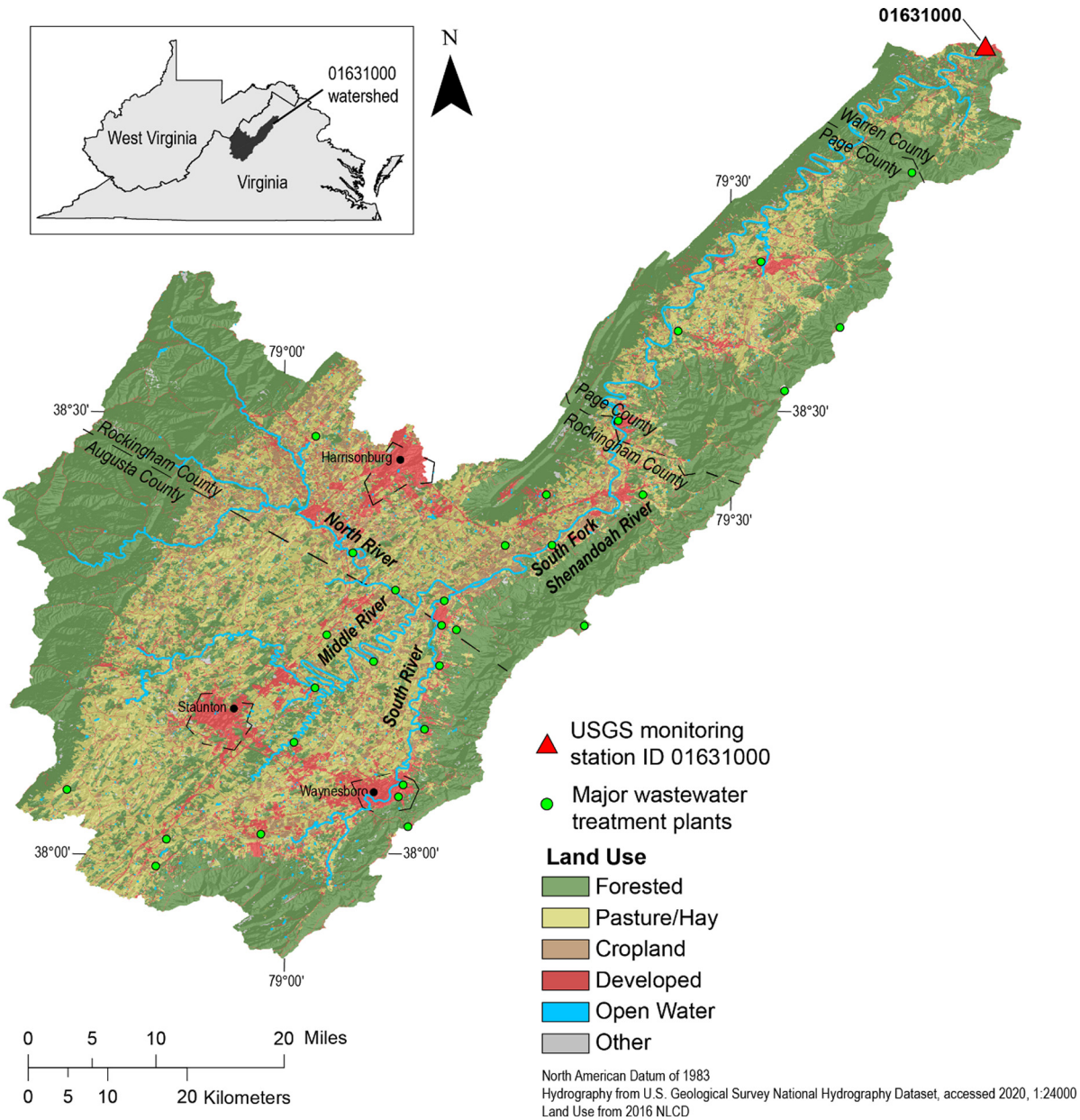

Fig. 2. Watershed map of the case study site, South Fork Shenandoah River at Front Royal, Virginia (USGS ID 01631000).

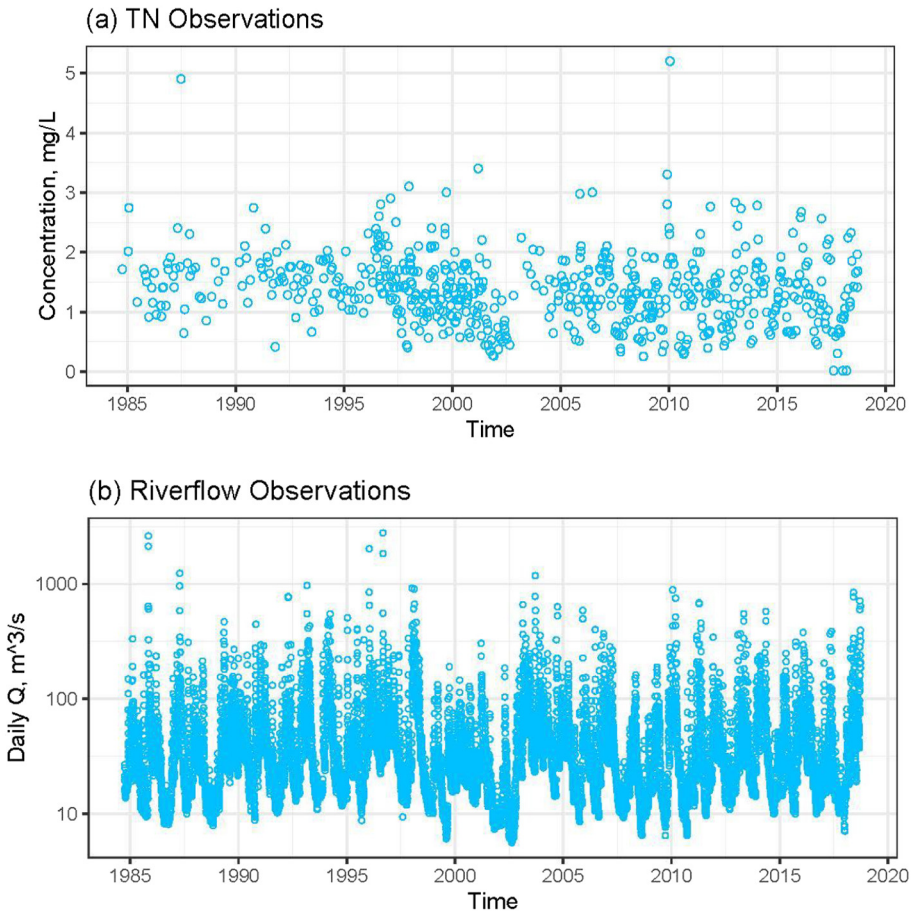

Fig. 3. Monitoring data of (a) TN concentration and (b) riverflow discharge (Q) collected at the case study site for water years 1985 through 2018.

the west, before joining the North Fork of the Shenandoah River. The monitoring station is located about 6 km upstream of this confluence. Carbonate geology is prevalent through this portion of Virginia and, because of the relatively flat topology, most of the aforementioned rivers flow over carbonate bedrock (King et al., 1974).

In terms of source inputs, the long-term (1985–2018) average values of TN from wastewater, atmospheric deposition, fertilizer, and manure are estimated to be 0.54, 4.96, 2.70, and 10.56 × 10^6 kg/yr, respectively (Chesapeake Bay Program, 2017). Clearly, manure is the most dominant source input in this watershed. Between 1985 and 2018, wastewater, atmospheric deposition, and fertilizer have decreased by 74%, 32%, and 24%, respectively, but manure has increased by 31% (Chesapeake Bay Program, 2017). Practices designed to reduce in-stream nutrient and sediment loads are used throughout the watershed and include approximately 500 km^2 of agricultural land enrolled in nutrient management, conservation tillage, cover crops, and pasture management as well approximately 23 km^2 of stormwater management on urban land (Chesapeake Bay Program, 2017).

In water years 1985 through 2018, the study site has daily riverflow data (12,419 values) but sparse TN concentration data (632 values) – see Fig. 3. The concentrations are generally below 3.5 mg/L and do not show a clear trend in this period. These monitoring data have been used to run WRTDS and the results are published in Moyer and Langland (2020).

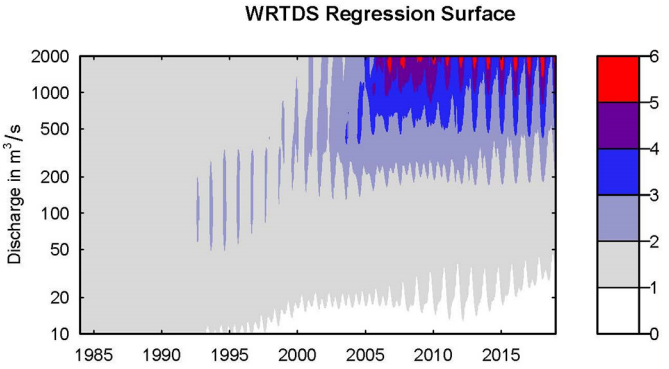

Fig. 4. WRTDS concentration regression surface for the case study for water years 1985 through 2018, showing estimated TN concentration (in mg/L) as functions of time and discharge.

3. Results and discussion

3.1. WRTDS FN trend

The WRTDS concentration regression surface was recreated for TN at the study site using the data in Moyer and Langland (2020) (Fig. 4), which reveals important patterns of the TN concentration between 1985 and 2018 that are hidden in Fig. 3a. Specifically, there is a decrease in TN concentration at relatively low-flow conditions (below ~50 m^3/s) throughout the record. By contrast, there is an increase in TN concentration at relatively high-flow conditions (above 200 m^3/s) in the latter part of the record.

The standard FN estimates were also reproduced for this case study (black line in Fig. 5). These flux estimates showed a period of decline (1985–2000), a period of increase (2000–2007), and another period of decline (2007–2018). Between water years 1985 and 2018, the overall

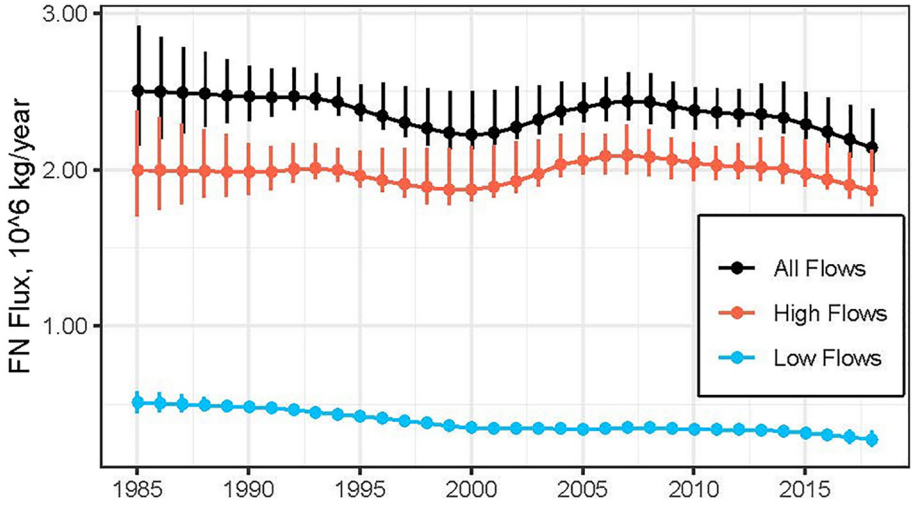

Fig. 5. Flow-normalized (FN) annual estimates of TN flux for the case study site for water years 1985 through 2018. The high-flow and low-flow FN estimates obtained from the FN_{2Q} approach sum exactly to the all-flow estimates obtained from the standard FN approach. Vertical bars represent the estimated 90% confidence intervals. In the text, the high-flow, low-flow, and all-flow FN flux estimates are called F_{FN_HIGH}, F_{FN_LOW}, and F_{FN_TOTAL}, respectively.

FN flux has decreased by 0.36×10^6 kg (−14.6%), which indicates an improving condition in TN at the case study site.

3.2. WRTDS FN_{2Q} trends

Estimates from the FN_{2Q} approach reveal new insights into the concentration dynamics under different flow conditions. For clarity, F_{FN_HIGH}, F_{FN_LOW}, and F_{FN_TOTAL} are used to represent the high-flow, low-flow, and all-flow FN flux estimates, respectively. (Note: $F_{FN\_TOTAL} = F_{FN}$; see Eq. (10).) In general, F_{FN_HIGH} (Fig. 5) showed a temporal pattern similar to F_{FN_TOTAL} (Fig. 5). By contrast, F_{FN_LOW} showed an overall decline, including a period of decline (1985–2000), a period of plateau (2000–2014), and another period of decline (2014–2018) (Fig. 5). Furthermore, Fig. 5 shows that the upward trend in F_{FN_TOTAL} in 2000–2007 was entirely driven by F_{FN_HIGH}. These broad patterns are consistent with interpretations from the concentration regression surface (Fig. 4).

A main feature of the FN_{2Q} approach is the ability to quantify FN fluxes and trends for different flow conditions. About 84% of F_{FN_TOTAL} was represented by F_{FN_HIGH} between 1985 and 2018. Over this 34-year period, F_{FN_HIGH} has decreased by 0.13×10^6 kg, whereas F_{FN_LOW} has decreased by 0.23×10^6 kg. Thus, the decline in F_{FN_LOW} accounted for 64% of the decline in F_{FN_TOTAL} (-0.36×10^6 kg), although F_{FN_LOW} only accounted for 16% of the mass of F_{FN_TOTAL} in this period. Therefore, the FN_{2Q} approach reveals the nuanced information that the 1985–2018 decline in TN flux at the study site is mostly accounted for by the low-flow conditions, although most of TN flux is contributed during the high-flow conditions. Furthermore, our uncertainty analysis quantified the likelihood of these trends. Specifically, the likelihood of a downward trend in F_{FN_LOW}, F_{FN_TOTAL}, and F_{FN_HIGH} is 99%, 92%, and 68%, respectively. According to rules published by Hirsch et al. (2015), these likelihood values correspond to "highly likely", "very likely", and "likely" downward trends, respectively.

Another utility of the FN_{2Q} approach is to characterize seasonal differences. For example, the annual estimates in Fig. 5 can be separated into growing (April 1 to September 30 in each year) and non-growing (October 1 to March 31 in each year) seasons (Fig. 6). For the low-flow class, the growing and non-growing seasons showed similar long-term trajectories and similar period-of-record declines – i.e., -0.11×10^6 kg and -0.12×10^6 kg, respectively. In fact, F_{FN_LOW} showed consistent declines in each calendar month between 1985 and 2018 (plot not shown). For the high-flow class, however, the two

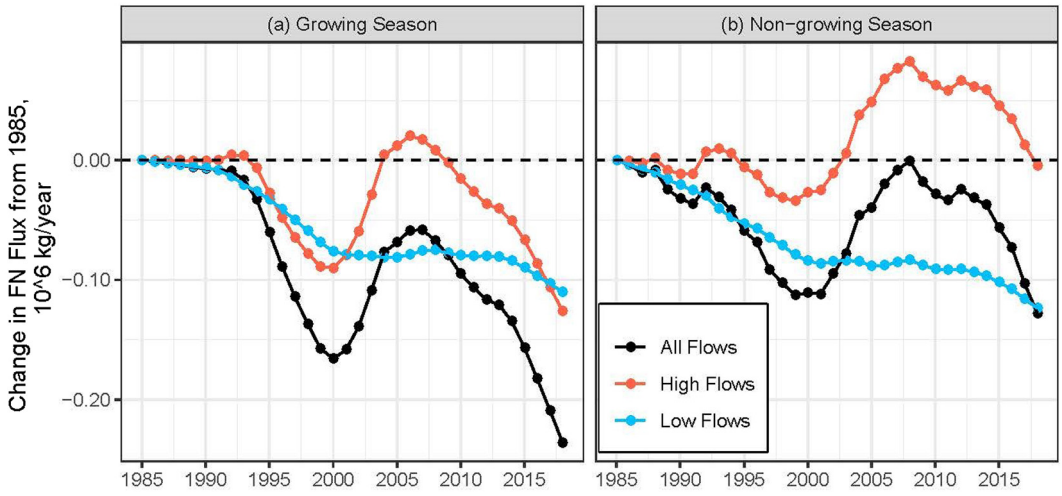

Fig. 6. Flow-normalized (FN) estimates of TN flux in (a) the growing season (April 1 – September 30) and (b) the non-growing season (October 1 – March 31) at the case study site for water years 1985 through 2018. To better compare the temporal patterns, all FN values have been subtracted by their corresponding values in 1985. Thus, all curves shown have a value of zero in 1985. In the text, the high-flow, low-flow, and all-flow FN flux estimates are called F_{FN_HIGH}, F_{FN_LOW}, and F_{FN_TOTAL}, respectively.

seasons were less similar. Specifically, the period-of-record decrease was much larger in the growing season (-0.13×10^6 kg) than the non-growing season (-0.004×10^6 kg) (Fig. 6). Thus, the period-of-record decrease in the total flux in the non-growing season was largely accounted for by the low-flow class, whereas the period-of-record decrease in the total flux in the growing season was attributed roughly equally to the low-flow and high-flow classes.

3.3. Factors affecting trends

FN_{2Q} is not only useful for characterizing river water-quality trends under different flows, but also guiding the direction of additional analysis for capturing the underlying drivers. Changing point source inputs, for example, due to upgraded wastewater treatment facilities, can be most evident on low-flow water-quality conditions, due to the absence of stormwater runoff carrying nonpoint source loads. Such changes in point source load may not be detected in F_{FN_TOTAL} because of contributions by F_{FN_HIGH}. In this regard, we assembled the TN loads discharged from major wastewater treatment facilities in the study watershed (Chesapeake Bay Program, 2017), which showed a dramatic decline of 0.56×10^6 kg (−77.6%) between water years 1985 and 2018 (Fig. 7a). We further compared these wastewater effluent loads with the FN and FN_{2Q} estimates. Clearly, F_{FN_LOW} was highly correlated with the wastewater effluent load ($R^2 = 0.72$), both of which showed strong declines in this period (Fig. 7d). By contrast, F_{FN_TOTAL} had a much weaker correlation with the wastewater effluent load ($R^2 = 0.25$; Fig. 7b), because F_{FN_HIGH} was very poorly correlated to the wastewater effluent load ($R^2 = 0.02$; Fig. 7c). As wastewater treatment plant upgrades are expected to result in year-round water-quality benefits, the consistent low-flow reductions in both growing and non-growing seasons offer further evidence for the role of point source reductions. In this regard, previous investigations reported large declines in wastewater and atmospheric deposition inputs but not in agricultural inputs (especially manure) during similar time periods (Chanat and Yang, 2018; Sabo, 2018). Consistent with our results, Sabo (2018) found that point sources were the best explanatory variable with respect to riverine N variability at the study site. However, the explanatory power of point sources was weak ($R^2 = 0.09$) because of competing effects by increased manure application rates and terrestrial N surplus. This is supported by our own analysis of source input data from Chesapeake Bay Program (2017), which showed that manure has increased by 31% in this watershed in the period of 1985–2018, whereas wastewater, atmospheric deposition, and fertilizer have decreased by 74%, 32%, and 24%, respectively, in the same period. These results demonstrate the utility of the FN_{2Q} approach for enhancing our capability to detect salient and important water-quality responses to management actions – i.e., the upgrades of treatment technology at wastewater treatment facilities in the study watershed have led to reductions of wastewater effluent load, which in turn have likely led to improvements of river water quality under low-flow conditions.

Water-quality patterns under high-flow conditions are more affected by changes in nonpoint source input. For this case study, we hypothesized that the spike in F_{FN_HIGH} of TN around 2007 was driven by the mobilization of particulate materials. This hypothesis is supported by a striking similarity between F_{FN_HIGH} of TN and F_{FN_HIGH} of suspended sediment (SS) (Fig. 8a–b), both of which peaked in 2007. The hypothesis can be further validated by splitting the TN flux to dissolved and particulate fractions, which are loosely represented by dissolved nitrate plus nitrite (NO_x) and TN – NO_x, respectively. Based on the FN_{2Q} approach, we found that F_{FN_HIGH} of NO_x has declined continually since 1994, without a spike around 2007 (Fig. 8c). By contrast, F_{FN_HIGH} of TN – NO_x showed a temporal pattern similar to that of TN, with a peak close to 2007 (Fig. 8d). These results support the conclusion that the high-flow spike of TN was likely caused by increased delivery of

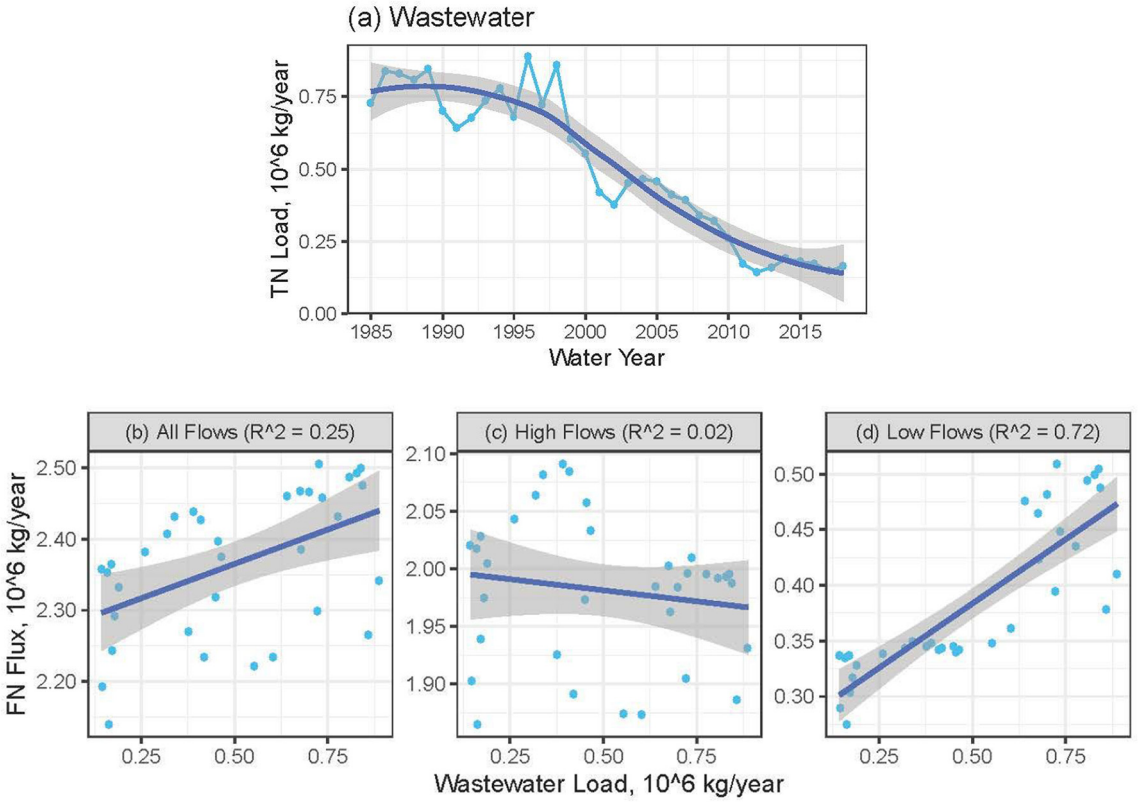

Fig. 7. (a) Annual TN loads discharged from major wastewater treament facilities in the study watershed for water years 1985 through 2018 and (b–d) its relation with the flow-normalized (FN) annual estimates of TN flux at the case study site. Note that the y-axis scale varies among panels (b)–(d). In the text, the high-flow, low-flow, and all-flow flux FN estimates are called F_{FN_HIGH}, F_{FN_LOW}, and F_{FN_TOTAL}, respectively. Data in panel (a) were retrieved from Chesapeake Bay Program (2017). Of the 261 wastewater facilities located in this watershed, only 29 have good-quality time series and their total loads are shown in panel (a) – see Fig. 2 for their locations.

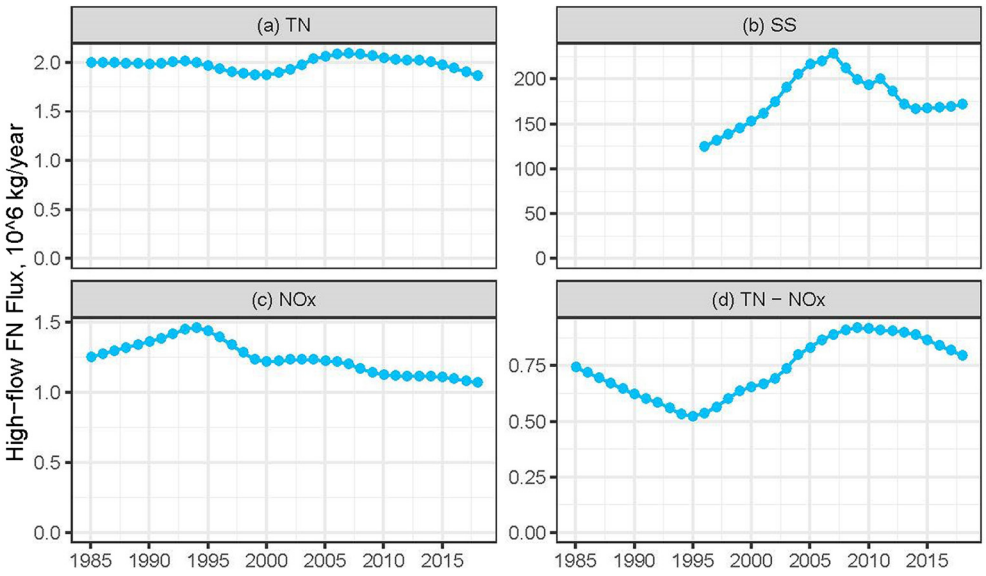

Fig. 8. Flow-normalized (FN) annual estimates of (a) TN flux, (b) SS flux, (c) NO_x flux, and (d) TN – NO_x flux under high-flow conditions at the case study site for water years 1985 through 2018. Note that the y-axis scale varies among panels. In the text, the high-flow FN flux estimates are called F_{FN_HIGH}.

particulate nitrogen associated with sediment transport. While a large fraction of nitrogen reaching Chesapeake Bay streams is contributed by groundwater nitrate (Bachman et al., 1998; Lindsey et al., 2003; Ator and Denver, 2012), these results highlight the importance of sediment mitigation strategies for achieving TN flux reductions.

3.4. Remarks on the applicability of FN_{2Q}

The FN_{2Q} approach (and the published code) can easily be applied to widely available river monitoring records to quantify water-quality trends under different flow conditions to enhance understanding of river water-quality dynamics. In this regard, we offer some remarks on the applicability and limitations of FN_{2Q}, which are consistent with WRTDS FN. First, it is certainly applicable to water-quality constituents other than TN. Second, this approach is applicable to records that contain left-censored (i.e., below-detection-limit) values (Moyer et al., 2012; Hirsch and De Cicco, 2015; Chanat et al., 2016). Third, FN_{2Q} is applicable to many monitoring stations in the United States and elsewhere, but it requires a complete record of daily discharge and a concentration record of 20+ years with 200+ samples is recommended (Hirsch et al., 2010). Fourth, this approach can be affected by the quantity and quality of high-flow concentration samples. The case study site, as well as other stations in the Chesapeake Bay nontidal monitoring network, have 12 regular monthly samples and eight targeted stormflow samples each year (Chanat et al., 2016). Compared to other approaches, WRTDS largely reduces the effect of high-flow samples on low-flow estimation due to its sample selection procedure. This feature is exploited by the FN_{2Q} approach, resulting in even higher confidence in the low-flow estimates. Fifth, FN_{2Q} is subject to the assumption of riverflow stationarity. That is, the distribution of flow on each calendar date has not significantly changed in the period of record. If this is violated, the generalized FN procedure should be engaged (Choquette et al., 2019). Sixth, FN_{2Q} may not be appropriate for small or flashy streams where riverflow is expected to rise and fall significantly in a single day.

Furthermore, we recognize two potential ways of modifying FN_{2Q} to accommodate users' specific needs. First, it can be modified to quantify fluxes and trends for flow classes that are different from those used here to accommodate users' own definition of low and high flows. However, we recommend at least several discharge values in each flow class in order to appropriately implement the FN computation. Second, it can be modified to quantify fluxes and trends for seasons that are different from those used here, which simply requires aggregating the estimated daily fluxes.

4. Conclusions

We demonstrated the utility of the FN_{2Q} approach for decomposing riverine water-quality trends into different flow classes. FN_{2Q} is not only useful for characterizing river water-quality trends under different flows, but also guiding the direction of additional analysis for capturing the underlying drivers, which can inform management strategies toward improving water quality. In the presented case study, the FN_{2Q} revealed several new insights into water-quality trends and drivers. First, F_{FN_TOTAL} of TN is mostly contributed by F_{FN_HIGH} in terms of mass; however, the decline in F_{FN_TOTAL} between 1985 and 2018 is mostly caused by the decline in F_{FN_LOW} (Fig. 5). Second, F_{FN_LOW} had similar declines between the growing and non-growing seasons, whereas F_{FN_HIGH} had a much larger decline in the growing season than the non-growing season (Fig. 6). Third, the decline in F_{FN_LOW} was highly correlated with the wastewater effluent loads, indicating that the upgrades of treatment technology at wastewater treatment facilities have likely led to the improvement of river water quality under low flows (Fig. 7). Lastly, F_{FN_HIGH} showed a spike around 2007, which was likely caused by increased delivery of particulate nitrogen associated with sediment transport (Fig. 8). More broadly, the FN_{2Q} approach (and the published code) can easily be applied to widely available river monitoring records to quantify water-quality trends under different flow conditions to enhance understanding of river water-quality dynamics.

CRediT authorship contribution statement

Qian Zhang: Conceptualization, Methodology, Software, Data curation, Formal analysis, Writing - original draft. **James S. Webber:** Conceptualization, Methodology, Software, Data curation, Formal analysis, Validation, Writing - review & editing. **Douglas L. Moyer:** Validation, Writing - review & editing. **Jeffrey G. Chanat:** Validation, Writing - review & editing.

Declaration of competing interest

The authors declare that they have no known competing financial interests or personal relationships that could have appeared to influence the work reported in this paper.

Acknowledgements

This work was supported by the U.S. Environmental Protection Agency (EPA/CBP Technical Support Grant No. 07-5-230480). Any use of trade, firm, or product names is for descriptive purposes only and does not imply endorsement by the U.S. Government. This is UMCES contribution number 5929.

Data availability

- The datasets of riverflow discharges and TN concentrations for the case study as well as the standard WRTDS model are available from Moyer and Langland (2020).
- The TN effluent data at the wastewater treatment facilities are available from Chesapeake Bay Program (2017).
- The R script for running the FN_{2Q} approach is available from Webber and Zhang (2020).
- Daily output from the FN_{2Q} approach is available for the case study site and other Chesapeake Bay nontidal monitoring stations from Webber and Zhang (2020).

References

Ator, S.W., Denver, J.M., 2012. Estimating contributions of nitrate and herbicides from groundwater to headwater streams, northern Atlantic Coastal Plain, United States. J. Am. Water Resour. Assoc. 48, 1075–1090. https://doi.org/10.1111/j.1752-1688.2012.00672.x.

Bachman, L.J., Lindsey, B., Brakebill, J., Powars, D.S., 1998. Ground-water discharge and base-flow nitrate loads of nontidal streams, and their relation to a hydrogeomorphic classification of the Chesapeake Bay Watershed, middle Atlantic coast. US Geological Survey Water-Resources Investigations Report 98-4059, Baltimore, MD , p. 71. http://pubs.usgs.gov/wri/wri98-4059/.

Boesch, D.F., 2019. Barriers and bridges in abating coastal eutrophication. Front. Mar. Sci. 6, 123. https://doi.org/10.3389/fmars.2019.00123.

Botter, M., Li, L., Hartmann, J., Burlando, P., Fatichi, S., 2020. Depth of solute generation is a dominant control on concentration-discharge relations. Water Resour. Res. 56. https://doi.org/10.1029/2019wr026695 e2019WR026695.

Burns, D.A., McDonnell, J.J., Hooper, R.P., Peters, N.E., Freer, J.E., Kendall, C., Beven, K., 2001. Quantifying contributions to storm runoff through end-member mixing analysis and hydrologic measurements at the Panola Mountain Research Watershed (Georgia, USA). Hydrol. Process. 15, 1903–1924. https://doi.org/10.1002/hyp.246.

Chanat, J.G., Yang, G., 2018. Exploring drivers of regional water-quality change using differential spatially referenced regression—a pilot study in the Chesapeake Bay watershed. Water Resour. Res. 54, 8120–8145. https://doi.org/10.1029/2017wr022403.

Chanat, J.G., Rice, K.C., Hornberger, G.M., 2002. Consistency of patterns in concentration-discharge plots. Water Resour. Res. 38, 1–10. https://doi.org/10.1029/2001WR000971.

Chanat, J.G., Moyer, D.L., Blomquist, J.D., Hyer, K.E., Langland, M.J., 2016. Application of a weighted regression model for reporting nutrient and sediment concentrations, fluxes, and trends in concentration and flux for the Chesapeake Bay Nontidal Water-Quality Monitoring Network, results through water year 2012. U.S. Geological Survey Scientific Investigations Report 2015–5133, Reston, VA, p. 76 https://doi.org/10.3133/sir20155133.

Chesapeake Bay Program, 2017. Chesapeake Assessment and Scenario Tool (CAST) Version 2017d.

Choquette, A.F., Hirsch, R.M., Murphy, J.C., Johnson, L.T., Confesor, R.B., 2019. Tracking changes in nutrient delivery to western Lake Erie: approaches to compensate for variability and trends in streamflow. J. Great Lakes Res. 45, 21–39. https://doi.org/10.1016/j.jglr.2018.11.012.

Cleveland, R.B., Cleveland, W.S., McRae, J.E., Terpenning, I., 1990. STL: a seasonal-trend decomposition procedure based on Loess. J. Off. Stat. 6, 3–73 (DOI).

Cohn, T.A., Delong, L.L., Gilroy, E.J., Hirsch, R.M., Wells, D.K., 1989. Estimating constituent loads. Water Resour. Res. 25, 937–942. https://doi.org/10.1029/WR025i005p00937.

Esterby, S.R., 1996. Review of methods for the detection and estimation of trends with emphasis on water quality applications. Hydrol. Process. 10, 127–149 10.1002/(sici)1099-1085(199602)10:2<127::Aid-hyp354>3.0.Co;2-8.

Fanelli, R.M., Blomquist, J.D., Hirsch, R.M., 2019. Point sources and agricultural practices control spatial-temporal patterns of orthophosphate in tributaries to Chesapeake Bay. Sci. Total Environ. 652, 422–433. https://doi.org/10.1016/j.scitotenv.2018.10.062.

Guo, D., Lintern, A., Webb, J.A., Ryu, D., Liu, S., Bende-Michl, U., Leahy, P., Wilson, P., Western, A.W., 2019. Key factors affecting temporal variability in stream water quality. Water Resour. Res. 55, 112–129. https://doi.org/10.1029/2018wr023370.

Hastie, T.J., Tibshirani, R.J., 1990. Generalized additive models. Chapam and Hall/CRC.

Hirsch, R.M., 2014. Large biases in regression-based constituent flux estimates: causes and diagnostic tools. J. Am. Water Resour. Assoc. 50, 1401–1424. https://doi.org/10.1111/jawr.12195.

Hirsch, R.M., De Cicco, L., 2015. User guide to Exploration and Graphics for RivEr Trends (EGRET) and dataRetrieval: R packages for hydrologic data (version 2.0, February 2015). U.S. Geological Survey Techniques and Methods Book 4, Chapter A10, Reston, VA, p. 93 https://doi.org/10.3133/tm4A10.

Hirsch, R.M., Slack, J.R., Smith, R.A., 1982. Techniques of trend analysis for monthly water quality data. Water Resour. Res. 18, 107–121. https://doi.org/10.1029/WR018i001p00107.

Hirsch, R.M., Alexander, R.B., Smith, R.A., 1991. Selection of methods for the detection and estimation of trends in water quality. Water Resour. Res. 27, 803–813. https://doi.org/10.1029/91wr00259.

Hirsch, R.M., Moyer, D.L., Archfield, S.A., 2010. Weighted regressions on time, discharge, and season (WRTDS), with an application to Chesapeake Bay river inputs. J. Am. Water Resour. Assoc. 46, 857–880. https://doi.org/10.1111/j.1752-1688.2010.00482.x.

Hirsch, R.M., Archfield, S.A., De Cicco, L.A., 2015. A bootstrap method for estimating uncertainty of water quality trends. Environ. Model Softw. 73, 148–166. https://doi.org/10.1016/j.envsoft.2015.07.017.

Keisman, J.L.D., Devereux, O.H., LaMotte, A.E., Sekellick, A.J., Blomquist, J.D., 2018. Manure and fertilizer inputs to land in the Chesapeake Bay watershed, 1950–2012. U.S. Geological Survey Scientific Investigations Report 2018–5022, Reston, VA, p. 37 https://doi.org/10.3133/sir20185022.

Kendall, M.G., 1975. Rank Correlation Methods. Oxford University Press, London, UK.

King, P.B., Beikman, H.M., Edmonston, G.J., 1974. Geologic Map of the United States (Exclusive of Alaska and Hawaii). U.S. Geological Survey https://doi.org/10.3133/70136641.

Lee, C.J., Hirsch, R.M., Schwarz, G.E., Holtschlag, D.J., Preston, S.D., Crawford, C.G., Vecchia, A.V., 2016. An evaluation of methods for estimating decadal stream loads. J. Hydro. 542, 185–203. https://doi.org/10.1016/j.jhydrol.2016.08.059.

Lee, C.J., Hirsch, R.M., Crawford, C.G., 2019. An evaluation of methods for computing annual water-quality loads. Scientific Investigations Report 2019–5084. U.S. Geological Survey, Reston, VA, p. 59 2328-0328.

Lindsey, B.D., Phillips, S.W., Donnelly, C.A., Speiran, G.K., Plummer, L.N., Böhlke, J.K., Focazio, M.J., Burton, W.C., 2003. Residence times and nitrate transport in ground water discharging to streams in the Chesapeake Bay watershed. U.S. Geological Survey Water-Resources Investigations Report 03-4035, New Cumberland, PA , p. 201. http://pa.water.usgs.gov/reports/wrir03-4035.pdf.

Lintern, A., Webb, J.A., Ryu, D., Liu, S., Bende-Michl, U., Waters, D., Leahy, P., Wilson, P., Western, A.W., 2018. Key factors influencing differences in stream water quality across space. WIREs Water 5. https://doi.org/10.1002/wat2.1260.

Lloyd, C.E.M., Freer, J.E., Collins, A.L., Johnes, P.J., Jones, J.I., 2014. Methods for detecting change in hydrochemical time series in response to targeted pollutant mitigation in river catchments. J. Hydro. 514, 297–312. https://doi.org/10.1016/j.jhydrol.2014.04.036.

Malone, T.C., Newton, A., 2020. The globalization of cultural eutrophication in the coastal ocean: causes and consequences. Front. Mar. Sci. 7, 670. https://doi.org/10.3389/fmars.2020.00670.

Manning, D.W.P., Rosemond, A.D., Benstead, J.P., Bumpers, P.M., Kominoski, J.S., 2020. Transport of N and P in U.S. streams and rivers differs with land use and between dissolved and particulate forms. Ecol. Appl. 30, e02130. https://doi.org/10.1002/eap.2130.

Moyer, D.L., Langland, M.J., 2020. Nitrogen, phosphorus, and suspended-sediment loads and trends measured at the Chesapeake Bay Nontidal Network stations: water years 1985-2018. U.S. Geological Survey Data Release https://doi.org/10.5066/P931M7FT.

Moyer, D.L., Hirsch, R.M., Hyer, K.E., 2012. Comparison of Two Regression-based Approaches for Determining Nutrient and Sediment Fluxes and Trends in the Chesapeake Bay Watershed. U.S. Geological Survey Scientific Investigations Report 2012–5244, Reston, VA. , p. 118. http://pubs.usgs.gov/sir/2012/5244/.

Murdoch, P.S., Shanley, J.B., 2006. Detection of water quality trends at high, median, and low flow in a Catskill Mountain stream, New York, through a new statistical method. Water Resour. Res. 42, 1–12. https://doi.org/10.1029/2004WR003892.

Murphy, J., Sprague, L., 2019. Water-quality trends in US rivers: exploring effects from streamflow trends and changes in watershed management. Sci. Total Environ. 656, 645–658. https://doi.org/10.1016/j.scitotenv.2018.11.255.

Murphy, R.R., Perry, E., Harcum, J., Keisman, J., 2019. A generalized additive model approach to evaluating water quality: Chesapeake Bay case study. Environ. Model Softw. 118, 1–13. https://doi.org/10.1016/j.envsoft.2019.03.027.

Oelsner, G.P., Stets, E.G., 2019. Recent trends in nutrient and sediment loading to coastal areas of the conterminous U.S.: insights and global context. Sci. Total Environ. 654, 1225–1240. https://doi.org/10.1016/j.scitotenv.2018.10.437.

Qian, S.S., Borsuk, M.E., Stow, C.A., 2000. Seasonal and long-term nutrient trend decomposition along a spatial gradient in the Neuse River watershed. Environ. Sci. Technol. 34, 4474–4482. https://doi.org/10.1021/es000989p.

Sabo, R.D., 2018. Shifting Inputs and Transformations of Nitrogen in Forested and Mixed Land Use Basins: Implications for Hydrologic Nitrogen Loss.

Seitzinger, S.P., Mayorga, E., Bouwman, A.F., Kroeze, C., Beusen, A.H.W., Billen, G., Van Drecht, G., Dumont, E., Fekete, B.M., Garnier, J., Harrison, J.A., 2010. Global river nutrient export: a scenario analysis of past and future trends. Glob. Biogeochem. Cycles 24. https://doi.org/10.1029/2009GB003587.

Sen, P.K., 1968. Estimates of the regression coefficient based on Kendall's tau. J. Am. Stat. Assoc. 63, 1379–1389. https://doi.org/10.1080/01621459.1968.10480934.

Sprague, L.A., Oelsner, G.P., Argue, D.M., 2017. Challenges with secondary use of multi-source water-quality data in the United States. Water Res. 110, 252–261. https://doi.org/10.1016/j.watres.2016.12.024.

Stackpoole, S.M., Stets, E.G., Clow, D.W., Burns, D.A., Aiken, G.R., Aulenbach, B.T., Creed, I.F., Hirsch, R.M., Laudon, H., Pellerin, B.A., Striegl, R.G., 2017. Spatial and temporal patterns of dissolved organic matter quantity and quality in the Mississippi River Basin, 1997–2013. Hydrol. Process. 31, 902–915. https://doi.org/10.1002/hyp.11072.

Stets, E.G., Sprague, L.A., Oelsner, G.P., Johnson, H.M., Murphy, J.C., Ryberg, K., Vecchia, A.V., Zuellig, R.E., Falcone, J.A., Riskin, M.L., 2020. Landscape drivers of dynamic

change in water quality of U.S. Rivers. Environ. Sci. Technol. 54, 4336–4343. https://doi.org/10.1021/acs.est.9b05344.
Stow, C.A., Cha, Y., Johnson, L.T., Confesor, R., Richards, R.P., 2015. Long-term and seasonal trend decomposition of Maumee River nutrient inputs to western Lake Erie. Environ. Sci. Technol. 49, 3392–3400. https://doi.org/10.1021/es5062648.
Webber, J.S., Zhang, Q., 2020. Chesapeake Bay nontidal network 1985 - 2018: Daily high-flow and low-flow concentration and load estimates. U.S. Geological Survey Data Release https://doi.org/10.5066/P9LBJEY1.
Yang, G., Moyer, D.L., 2020. Estimation of nonlinear water-quality trends in high-frequency monitoring data. Sci. Total Environ. 715, 136686. https://doi.org/10.1016/j.scitotenv.2020.136686.
Zhang, Q., Blomquist, J.D., 2018. Watershed export of fine sediment, organic carbon, and chlorophyll-a to Chesapeake Bay: spatial and temporal patterns in 1984–2016. Sci. Total Environ. 619-620, 1066–1078. https://doi.org/10.1016/j.scitotenv.2017.10.279.
Zhang, Q., Brady, D.C., Boynton, W.R., Ball, W.P., 2015. Long-term trends of nutrients and sediment from the nontidal Chesapeake watershed: an assessment of progress by river and season. J. Am. Water Resour. Assoc. 51, 1534–1555. https://doi.org/10.1111/1752-1688.12327.
Zhang, Q., Ball, W.P., Moyer, D.L., 2016a. Decadal-scale export of nitrogen, phosphorus, and sediment from the Susquehanna River basin, USA: analysis and synthesis of temporal and spatial patterns. Sci. Total Environ. 563-564, 1016–1029. https://doi.org/10.1016/j.scitotenv.2016.03.104.
Zhang, Q., Harman, C.J., Ball, W.P., 2016b. An improved method for interpretation of riverine concentration-discharge relationships indicates long-term shifts in reservoir sediment trapping. Geophys. Res. Lett. 43, 10,215–210,224. https://doi.org/10.1002/2016gl069945.
Zhi, W., Li, L., 2020. The shallow and deep hypothesis: subsurface vertical chemical contrasts shape nitrate export patterns from different land uses. Environ. Sci. Technol. https://doi.org/10.1021/acs.est.0c01340.